

Published in final edited form as:

*J Cell Physiol.* 2008 November ; 217(2): 319–327. doi:10.1002/jcp.21503.

## Age-dependent Impairment of HIF-1 $\alpha$ Expression in Diabetic Mice: Correction with Electroporation-facilitated Gene Therapy Increases Wound Healing, Angiogenesis, and Circulating Angiogenic Cells

Lixin Liu<sup>1</sup>, Guy P. Marti<sup>1</sup>, Xiaofei Wei<sup>2</sup>, Xianjie Zhang<sup>1</sup>, Huafeng Zhang<sup>2</sup>, Ye V. Liu<sup>2</sup>, Manuel Nastai<sup>1</sup>, Gregg L. Semenza<sup>2,\*</sup>, and John W. Harmon<sup>1</sup>

<sup>1</sup>Section of Surgical Sciences, Johns Hopkins University School of Medicine, Baltimore, MD

<sup>2</sup>Vascular Program, Institute for Cell Engineering; Departments of Pediatrics, Medicine, Oncology, Radiation Oncology; and the McKusick-Nathans Institute of Genetic Medicine, The Johns Hopkins University School of Medicine, Baltimore, MD

### Abstract

Wound healing is impaired in elderly patients with diabetes mellitus. We hypothesized that age-dependent impairment of cutaneous wound healing in *db/db* diabetic mice: (a) would correlate with reduced expression of the transcription factor hypoxia-inducible factor 1 $\alpha$  (HIF-1 $\alpha$ ) as well as its downstream target genes; and (b) could be overcome by HIF-1 $\alpha$  replacement therapy. Wound closure, angiogenesis, and mRNA expression in excisional skin wounds were analyzed and circulating angiogenic cells were quantified in *db/db* mice that were untreated or received electroporation-facilitated HIF-1 $\alpha$  gene therapy. HIF-1 $\alpha$  mRNA levels in wound tissue were significantly reduced in older (4–6 months) as compared to younger (1.5–2 months) *db/db* mice. Expression of mRNAs encoding the angiogenic cytokines vascular endothelial growth factor (VEGF), angiopoietin 1 (ANGPT1), ANGPT2, platelet derived growth factor B (PDGF-B), and placental growth factor (PLGF) was also impaired in wounds of older *db/db* mice. Intradermal injection of plasmid gWIZ-CA5, which encodes a constitutively active form of HIF-1 $\alpha$ , followed by electroporation, induced increased levels of HIF-1 $\alpha$  mRNA at the injection site on day 3 and increased levels of VEGF, PLGF, PDGF-B, and ANGPT2 mRNA on day 7. Circulating angiogenic cells in peripheral blood increased 10-fold in mice treated with gWIZ-CA5. Wound closure was significantly accelerated in *db/db* mice treated with gWIZ-CA5 as compared to mice treated with empty vector. Thus, HIF-1 $\alpha$  gene therapy corrects the age-dependent impairment of HIF-1 $\alpha$  expression, angiogenic cytokine expression, and circulating angiogenic cells that contribute to the age-dependent impairment of wound healing in *db/db* mice.

### Keywords

Aging; Angiogenesis; Diabetes; Wound Healing

---

\*Address correspondence to Gregg L. Semenza, M.D., Ph.D., Broadway Research Building, Suite 671, 733 North Broadway, Baltimore, MD 21205. Tel: 410-955-1619; Fax: 443-287-5618; E-mail: E-mail: gsemenza@jhmi.edu.

## Introduction

Impaired wound healing is an age-dependent manifestation of diabetes mellitus. Aging and diabetes have each been shown to impair wound healing (Davidson, 1998; Gosain and DiPietro, 2004) and the combination of age and diabetes has a synergistic effect (Brem et al., 2007). Contributing factors include abnormal inflammatory responses, reduced granulation tissue deposition, and decreased angiogenesis in diabetic wounds. Impaired expression of angiogenic growth factors, including vascular endothelial growth factor (VEGF) and placental growth factor (PLGF), plays an important role in the impairment of wound healing that is associated with diabetes (Frank et al., 1995; Cianfarani et al., 2006). However, the molecular mechanisms underlying such defects have not been fully elucidated.

Angiogenic growth factors activate endogenous endothelial cells and also recruit circulating angiogenic cells (CACs), a term used here to denote a heterogeneous population of cells that participate in various aspects of angiogenesis. They include endothelial progenitor cells, which incorporate into the endothelium of new or remodeling vessels, as well as myeloid, mesenchymal, and hematopoietic stem cells, which may promote vascular growth and remodeling through the production of angiogenic cytokines (Asahara et al., 1999; Grant et al., 2002; Rehman et al., 2003; Kinnaird et al., 2004; Grunewald et al., 2006; Jin et al., 2006; Yoder et al., 2007). CACs are released from blood vessels, bone marrow, and other sites in response to the production of angiogenic cytokines at the site of tissue wounding. Following mobilization into the circulation, CACs home to the wound, where they participate in angiogenesis. Decreased levels of CACs are observed in patients with type 1 and type 2 diabetes and, in the latter, reduced CACs are associated with peripheral vascular disease (Loomans et al., 2004; Fadini et al., 2005, 2006).

Hypoxia-inducible factor 1 (HIF-1) is a transcriptional activator that promotes angiogenesis (Pugh and Ratcliffe, 2003; Brahimi-Horn and Pouyssegur, 2007; Semenza, 2007). HIF-1 is a heterodimeric protein that is composed of a constitutively expressed HIF-1 $\beta$  subunit and an O<sub>2</sub>-regulated HIF-1 $\alpha$  subunit (Wang et al., 1995). Under normoxic conditions the HIF-1 $\alpha$  subunit is ubiquitinated and subsequently degraded, whereas under hypoxic conditions, HIF-1 $\alpha$  accumulates, dimerizes with HIF-1 $\beta$ , and activates the expression of target genes (Cummins and Taylor, 2005). Among the known HIF-1 target genes are those encoding angiogenic growth factors and cytokines implicated in wound healing, including VEGF, PLGF, angiopoietins (ANGPT1, ANGPT2), and platelet-derived growth factor B (PDGF-B) (Kelly et al., 2003; Patel et al., 2005; Bosch-Marcé et al., 2007). HIF-1 $\alpha$  expression is also induced under normoxic conditions when cells are stimulated with growth factors, inflammatory cytokines, lactate, or prostaglandins (Laughner et al., 2001; Fukuda et al., 2002, 2003; Stiehl et al., 2002; Treins et al., 2002; Hunt et al., 2007).

HIF-1 $\alpha$  expression is induced during wound healing (Elson et al., 2000; Albina et al., 2001) and is impaired in dermal fibroblasts and endothelial cells exposed to increased glucose concentrations (Catrina et al., 2004). HIF-1 $\alpha$  expression was impaired during the healing of large cutaneous wounds in young *db/db* mice and HIF-1 $\alpha$  gene therapy accelerated wound healing and angiogenesis in this model (Mace et al., 2007). Because impaired healing is a major cause of morbidity and mortality in the elderly population, we specifically analyzed the effect of aging on the expression of HIF-1 $\alpha$  and angiogenic growth factors in *db/db* mice. In addition, we investigated the use of electroporation-facilitated cutaneous DNA transfection, which significantly increases reporter gene expression *in vivo* (Lee et al., 2004; Byrnes et al., 2004; Pavselyj et al., 2005; Lin et al., 2006). This technique was utilized to transduce a plasmid encoding a constitutively active form of HIF-1 $\alpha$ , designated HIF-1 $\alpha$ CA5, which induces HIF-1-regulated gene expression even under non-hypoxic conditions (Kelly et al., 2003; Patel et al., 2005; Bosch-Marcé et al., 2007). We focused on the connection between HIF-1,

angiogenic cytokine expression, mobilization of CACs, blood vessel formation, and wound healing.

## Materials and Methods

### Plasmids

Plasmid pCEP4 was obtained from Invitrogen (Carlsbad, CA); plasmids gWIZ and gWIZ-luc were obtained from Genlantis (San Diego, CA). The nucleotide sequence encoding HIF-1 $\alpha$ CA5 was excised from pCEP4/HIF-1 $\alpha$ CA5 by digestion with EcoRV and BamHI and inserted into EcoRV/BamHI-digested gWIZ vector. HIF-1 $\alpha$ CA5 contains a deletion (amino acids 392–520) and missense mutations (Pro567Thr, Pro658Gln) that render the protein resistant to O<sub>2</sub>-dependent degradation (Kelly et al. 2003). All plasmids were purified using an endotoxin-free plasmid purification kit (Qiagen, Valencia, CA) following manufacturer's instructions.

### Cell culture and transient transfection assays

HEK-293T cells were obtained from ATCC (Manassas, VA) and maintained in DMEM supplemented with 10% fetal bovine serum (Hyclone, Logan, UT) in a humidified incubator at 37°C with 95% air/5% CO<sub>2</sub>. For RNA expression assays, 1×10<sup>6</sup> HEK-293T cells were seeded in a 6-cm dish and transfected with 1 μg of plasmid DNA using Fugene 6 (Roche, Indianapolis, IN). Total RNA was extracted 24 h after transfection and assayed by quantitative real-time reverse transcription-polymerase chain reaction (qRT-PCR). For the luciferase reporter assays, HEK-293T cells were seeded onto 48-well plates at 4.5×10<sup>4</sup> cells per well and transfected using Fugene-6 with the following plasmids: pSV-Renilla (1 ng), HIF-1-dependent firefly luciferase reporter p2.1 (10 ng), and expression vector (10 ng). Cells were lysed 24 h after transfection, and firefly:Renilla luciferase activities were determined with a multi-well luminescence reader (PerkinElmer) using the Dual-Luciferase Reporter Assay System (Promega). Three independent transfections were performed.

### Animal protocols

Animal procedures were approved by the Johns Hopkins University Animal Care and Use Committee. Female BKS.Cg-m<sup>+/+</sup>Lepr<sup>db</sup>/J mice were obtained from The Jackson Laboratory (Bar Harbor, ME). During experiments, the animals were housed one per cage, maintained under controlled environmental conditions (12 h:12 h light:dark cycle, temperature approximately 23°C), and provided with standard laboratory food and water ad libitum, with the exception of the 12-h fast prior to glucose measurements, when only water was given. Fasting glucose was measured using a Glucometer (Roche Diagnostics Corp., Indianapolis, IN). Hb A<sub>1c</sub> was measured using an A1cNow test kit (Metrika, Sunnyvale, CA).

Mice were anesthetized with ketamine hydrochloride (100 mg/kg) and xylazine (10 mg/kg), the dorsum was shaved, and two or four full-thickness circular excisional wounds were created using a 5-mm biopsy punch (Acuderm, Ft. Lauderdale, FL). Wounds were left undressed and animals were housed individually. In treatment studies, mice subsequently received intradermal injections of plasmid (25 μg) or vehicle at two sites on both sides of the wound. The resulting skin blebs confirmed intradermal delivery of the solution. Animals were electroporated at the site of injection within 2 min after plasmid injection using a square wave electroporator (ECM 830, BTX Genetronics, San Diego, CA). A custom-designed pin electrode, consisting of two 10-mm rows of parallel acupuncture needles separated by 5 mm was used to apply the electroporation current. Ten square wave pulses were administered at an amplitude of 400 V for a duration of 20 msec, and an interval between pulses of 125 msec.

### Wound area measurements

On days 0, 5, 7, and 10, the wound eschar was carefully removed and the unepithelialized wound border was traced *in situ* onto clear acetate paper by two examiners who were blinded to the experimental conditions. Images were digitized at 600 dpi (Paperport 6000, Visioneer, Fremont, CA) and wound areas were calculated (in pixels) using image analysis software (Scion Image, Frederick, MD).

### RNA isolation and qRT-PCR assays

Total RNA was extracted from mouse wound tissue with TRIzol (Invitrogen, Frederick, MD) and treated with DNase I (Ambion, Austin, TX) according to the manufacturer's protocol. Ten  $\mu\text{g}$  of total RNA was used for reverse transcription with the iScript cDNA Synthesis system (BioRad Laboratories, Hercules, CA). Real-time PCR was performed using iQ SYBR Green Supermix and the iCycler Real-Time PCR Detection System (BioRad). For each primer pair (Bosch-Marcé et al., 2007), annealing temperature was optimized by gradient PCR. The fold change in expression of each target mRNA (VEGF, PLGF, ANGPT1, ANGPT2, and PDGFB) relative to hypoxanthine phosphoribosyltransferase 1 (HPRT1) mRNA was calculated based on the threshold cycle ( $C_T$ ) for amplification as  $2^{\Delta(\Delta C_T)}$ , where  $\Delta C_T = C_{T,\text{target}} - C_{T,\text{HPRT1}}$ .

### *In vivo* luciferase imaging

Animals were sedated and then received a 140- $\mu\text{l}$  intraperitoneal injection of D-luciferin (15 mg/ml in PBS). A photograph was taken and bioluminescent images were acquired using a cooled charge-coupled device camera (IVIS, Xenogen, Alameda, CA). Luminescent images were taken 20 min after luciferin administration, during which time the light emission is in plateau phase. The bioluminescent image was overlaid onto the photograph of each animal, and the light emission, corrected for background luminescence, was calculated for each injection site using image analysis software (Living Image, Xenogen, Alameda, CA). The intensity of luminescence is represented by a color scale corresponding to the total number of photons emitted per second from 1  $\text{cm}^2$  of tissue. The color scale is standardized for all output images (minimum:  $1.5 \times 10^4$  photons/sec/ $\text{cm}^2$ ; maximum:  $1 \times 10^6$  photons/sec/ $\text{cm}^2$ ).

### Peripheral blood mononuclear cell culture assay

As described previously (Bosch-Marcé et al., 2001), peripheral blood mononuclear cells were isolated by Histopaque-1083 (Sigma) density gradient centrifugation. Residual red blood cells were lysed by ammonium chloride treatment. Mononuclear cells were seeded on 96-well plates coated with rat vitronectin at  $1.5 \times 10^6$  cells/ $\text{cm}^2$  and cultured in endothelial basal medium 2 supplemented with EGM-2-MV SingleQuots (Lonza, Walkersville, MD). After 4 days in culture, the cells were incubated with 1,1'-dioctadecyl-3,3',3'-tetramethylindocarbocyanine (DiI)-labeled acetylated low-density lipoprotein (LDL) (Invitrogen) in the media at a concentration of 2.4  $\mu\text{g}/\text{ml}$  at 37 °C for 2 h. The cells were then fixed with 4% paraformaldehyde for 10 min, incubated with fluorescein isothiocyanate (FITC)-labeled *Bandeira simplicifolia* agglutinin-1 (BS-1 lectin; Sigma) at a concentration of 10  $\mu\text{g}/\text{ml}$  for 1 h, and counterstained with 4',6-diamidino-2-phenylindole (Invitrogen). Cells staining positive for both DiI and FITC were counted under a fluorescence microscope.

### Immunohistochemistry

On day 7, wounds were excised, fixed in 10% formalin or IHC zinc fixative (BD Pharmingen, San Diego, CA), embedded in paraffin, and 5- $\mu\text{m}$ -thick sections were prepared. To prevent nonspecific binding, 100  $\mu\text{l}$  of blocking solution containing 2% normal rabbit serum was applied for 30 minutes, and then 100  $\mu\text{l}$  of rat-anti-mouse CD31 antibody (BD Pharmingen, Franklin Lakes, NJ) was applied to the sections at 1:50 dilution for 1 h at room temperature. The sections were then incubated with biotinylated secondary antibody (Vector Laboratories,

Burlingame, CA) at 1:500 dilution. Streptavidin-biotin-horseradish peroxidase (Vector Laboratories) was used for signal amplification and diaminobenzidine (Vector Laboratories) was used for staining. Counter-staining was performed with hematoxylin for 30 sec. 3% H<sub>2</sub>O<sub>2</sub> (Fisher Scientific, Fair Lawn, NJ) was used for blocking endogenous peroxidase activity. Histologic sections from each wound were independently analyzed and graded by two examiners who were blinded as to the identity of each sample. Vessel morphometrics were performed by obtaining a photomicrograph of the center of each wound immediately beneath the epithelium at 200x power with an IX70 microscope (Olympus Inc., Orangeburg, NY) and CD color camera M-852 (Micro-Technica, Tokyo, Japan), followed by image analysis using Image-Pro-Plus software (Media Cybernetics, Bethesda, MD). Appropriate filters were applied uniformly to capture the antibody staining. The number of vessels was determined by manual counting. Vessel area was determined by the software program.

### Statistical analysis

Results are presented as mean  $\pm$  standard error of the mean. Differences in means between groups were analyzed for significance using Student's t-test or ANOVA as appropriate.

## Results

### Impairment of wound healing in young and old diabetic mice

*db/db* mice are homozygous for a loss-of-function mutation in the *Lepr* gene encoding the leptin receptor and exhibit characteristics of adult onset (type 2) diabetes including hyperglycemia and obesity. To compare the wound healing characteristics of 2-month-old *db/db* mice with their heterozygous (*db/+*), non-diabetic littermates, two 5-mm-diameter excisional wounds were created on the left and right dorsum of each animal, and the unepithelialized wound areas were measured on day 9. The mean wound area for the diabetic mice was 6-fold greater than their non-diabetic littermates (Fig. 1A), indicating significantly impaired cutaneous wound healing in *db/db* mice ( $P < 0.01$ , Student's t-test).

To analyze the effect of aging on wound healing in diabetes, 2- and 21-month-old *db/db* mice were given two full thickness 5-mm wounds. On day 9, the wound areas of 2-month-old mice were 3-fold smaller than those of 21-month-old mice (Fig. 1B), indicating that aging significantly impaired wound healing in *db/db* mice ( $P < 0.01$ , Student's t-test). These results are consistent with results obtained using other wound models in these mice (Werner et al., 1994; Wetzler et al., 2000; Brem et al., 2007; Michaels et al., 2007).

### Effect of aging on glucose homeostasis

Glycosylated hemoglobin levels reflect long-term loss of glycemic control (Selvin et al., 2004). A previous study reported increased fasting blood glucose and HbA<sub>1C</sub> levels in 16-month-old as compared to 2-month-old *db/db* mice (3). We measured blood glucose and HbA<sub>1C</sub> levels in young (2-month-old;  $n = 7$ ) and mature (6-month-old;  $n = 18$ ) *db/db* mice. Compared to the young mice, the mature mice showed a significantly higher ( $P < 0.01$ , Student's t-test) glucose level ( $583 \pm 15$  vs  $499 \pm 48$  mg/dl) and percentage of glycosylated hemoglobin ( $10.5 \pm 0.4\%$  vs  $5.6 \pm 0.3\%$ ), indicating that the progressive impairment of glucose homeostasis with age is already demonstrable in 6-month-old *db/db* mice.

### Expression of mRNAs encoding HIF-1 $\alpha$ and angiogenic cytokines after wounding

We next tested the hypothesis that the age-related impairment in cutaneous wound healing in diabetic mice was associated with impaired expression of mRNAs encoding HIF-1 $\alpha$  and angiogenic growth factors. Two excisional wounds were created on the dorsum of young (1.5–2 month-old) and mature (4–6 month-old) mice, and skin samples were harvested 3 or 5 days

after wounding (n = 3 mice per time point per age group). Total RNA isolated from wound tissue was subjected to qRT-PCR to assess the levels of HIF-1 $\alpha$ , PLGF, PDGF-B, VEGF, ANGPT1 and ANGPT2 mRNA. Baseline HIF-1 $\alpha$  mRNA levels were 26 $\pm$ 7 fold higher in young as compared to mature *db/db* mice (Fig. 2A). HIF-1 $\alpha$  mRNA levels were significantly greater in young as compared to mature *db/db* mice on day 5 after wounding (168 $\pm$ 55 vs 13 $\pm$ 4; Fig. 2A). Expression of mRNAs encoding the angiogenic cytokines VEGF, ANGPT1, ANGPT2, PDGF-B and PLGF was also significantly increased in day 5 wounds of young *db/db* mice, whereas little or no change in expression was observed in mature *db/db* mice (Fig. 2B–F). These results demonstrate an age-related impairment in the expression of mRNAs encoding HIF-1 $\alpha$  and angiogenic cytokines in wounds of *db/db* mice.

### Construction and *ex vivo* testing of expression vector gWIZ-CA5

In order to engineer a high efficiency vector for expression of HIF-1 $\alpha$  *in vivo*, the human HIF-1 $\alpha$ CA5 DNA sequence was excised from pCEP4-CA5 and cloned into the gWIZ expression vector, which utilizes a modified cytomegalovirus promoter and a rabbit  $\beta$ -globin polyadenylation signal for high-level expression. Plasmid pCEP4-CA5, gWIZ-CA5, or empty vector was transfected into human HEK-293T cells and 24 hours later HIF-1 $\alpha$  mRNA levels were analyzed by qRT-PCR using primers that amplified both endogenous HIF-1 $\alpha$  and HIF-1 $\alpha$ CA5 (Fig. 3A). The results were normalized to those obtained from cells without transfection. The increase in HIF-1 $\alpha$  mRNA levels in gWIZ-CA5 transfected cells was 10 times greater (33.6 fold increase over non-transfected cells) when compared to the increase observed in pCEP4-CA5 transfected cells (3.3 fold).

The ability of gWIZ-CA5 to activate transcription of a HIF-1-dependent reporter gene was assessed next. HEK-293T cells were co-transfected with the HIF-1-dependent firefly luciferase reporter p2.1, which contains a 68-bp hypoxia response element from the human *ENO1* gene (Semenza et al., 1996), and pCEP4 or gWIZ expression vector encoding HIF-1 $\alpha$ CA5 or the respective empty vector. Reporter gene activity induced by gWIZ-CA5 was 9 times greater (86.4 $\pm$ 4.2 fold) than that induced by pCEP4-CA5 (9.5 $\pm$ 0.8 fold) (Fig. 3B). Thus, gWIZ-CA5 was chosen for the subsequent *in vivo* experiments based on its high level of HIF-1 $\alpha$  expression and HIF-1-dependent gene transcription.

### Electroporation-facilitated cutaneous gene transduction

Electroporation is the application of an electric field across cells in order to permeabilize the cell membrane and allow the entry of charged macromolecules such as DNA (Ferguson et al., 2005). Cutaneous gene delivery is enhanced using electroporation following intradermal injection of naked DNA (Chesnoy and Huang, 2002; Byrnes et al., 2004; Marti et al., 2004). We compared electroporation protocols with different electrical parameters using bioluminescence imaging after gWIZ-luc transduction into the skin of *db/db* mice (Fig. 4A). The electroporation protocol at 400V (10 square wave pulses, 400 V/cm amplitude, 20 ms duration, 125 msec interval) had the highest efficiency (Fig. 4B) and was chosen for subsequent experiments.

To test the effect of gWIZ-CA5 *in vivo*, plasmid DNA was injected intradermally (4 sites per animal with 50  $\mu$ g per site) in 6-month-old *db/db* mice, followed by electroporation. Skin samples from the injection sites were harvested 3, 7, 14, or 21 days later. Total RNA was extracted and analyzed by qRT-PCR using primers that amplified both mouse HIF-1 $\alpha$  and human HIF-1 $\alpha$ CA5 sequences. The HIF-1 $\alpha$  mRNA levels were maximal on day 3 (696-fold increase over non-transfected control) and were still elevated relative to non-transfected mice at the last time point tested (26-fold increase on day 21) (Fig. 5A). Empty vector injection and electroporation did not increase HIF-1 $\alpha$  levels (data not shown). VEGF, PLGF, PDGF-B, and ANGPT2 mRNA levels were elevated on day 7 (Fig. 5B). These results demonstrate that gWIZ-

CA5 increases HIF-1 $\alpha$  mRNA levels, leading to increased expression of genes encoding angiogenic growth factors/cytokines in cutaneous tissue of diabetic mice.

### Mobilization of circulating angiogenic cells after gWIZ-CA5 electroporation

To test whether HIF-1 $\alpha$  could mobilize CACs into the peripheral blood of diabetic mice, we transfected *db/db* mice with gWIZ-CA5 or empty vector control (gWIZ-EV), at 4 sites per animal with 50  $\mu$ g per site, followed by electroporation. On day 3 after electroporation, peripheral blood mononuclear cells were isolated, cultured under endothelial growth conditions for 4 days, and the number of cells which internalized DiI-labeled acetylated LDL and bound FITC-labeled BS-1 lectin were determined. The mean CAC count in the gWIZ-CA5-transfected group was increased 11-fold over the empty vector-transfected group (Fig. 6), demonstrating that cutaneous HIF-1 $\alpha$  overexpression is sufficient to mobilize CACs in diabetic mice.

### Accelerated wound closure and angiogenesis after electroporation of gWIZ-CA5

To test the effect of gWIZ-CA5 DNA transduction on wound healing, four wounds were created on the dorsum of 4-month-old *db/db* mice with a 5-mm biopsy punch. We performed intradermal injection of 25  $\mu$ g of gWIZ-CA5 or gWIZ-EV on two sides cephalad and caudal to the wound, followed by electroporation. The wound area was measured on days 0, 5, 7 and 10. Starting on day 5, wound area in the gWIZ-CA5 treated group (n = 48 wounds) was significantly reduced (p<0.001) compared to that of the empty vector treated group (n=20 wounds) (Fig. 7A). On day 10, only 12% of the wounds were  $\geq$ 95% closed in the empty vector-treated group, whereas 60% of wounds were  $\geq$ 95% closed in the gWIZ-CA5-treated group, demonstrating that the rate of wound closure was significantly increased after HIF-1 $\alpha$ CA5 transduction (Fig. 7B).

Using the same protocol, angiogenesis in day 7 wounds from *db/db* mice treated with gWIZ-CA5 or gWIZ-EV was analyzed by immunohistochemistry using an antibody against the endothelial cell-specific marker PECAM-1 (CD31). PECAM-1-positive vessel counts (Fig. 8A and 8B) and total vessel area (Fig. 8A and 8C) were both significantly increased in wounds from gWIZ-CA5-treated as compared to gWIZ-EV-treated mice.

## Discussion

In this study we have shown that aging of *db/db* mice is associated with progressive impairment of glucose homeostasis, wound healing, and the expression of mRNAs encoding the angiogenic cytokines VEGF, PLGF, ANGPT1, ANGPT2, and PDGFB in response to wounding. Associated with these defects, we have demonstrated impaired expression of HIF-1 $\alpha$  mRNA. HIF-1 has been shown to directly activate transcription of the *VEGF* gene (Forsythe et al., 1996) and to positively regulate expression of PLGF, ANGPT2, and PDGFB mRNA, as demonstrated by both gain-of-function and loss-of-function experimental approaches (Kelly et al., 2003; Patel et al., 2005; Bosch-Marcé et al., 2007). Taken together, these findings suggest that impaired expression of HIF-1 $\alpha$  plays an important pathogenic role in the impairment of angiogenic gene expression in aging diabetic mice.

As a means of correcting the deficient expression of HIF-1 $\alpha$  in *db/db* mice, we utilized electroporation-facilitated plasmid DNA transduction and demonstrated high-level expression of HIF-1 $\alpha$ CA5. Furthermore, in contrast to the transient induction of HIF-1 $\alpha$  mRNA that was observed after adenovirus-mediated HIF-1 $\alpha$ CA5 gene transduction (Kelly et al., 2003), HIF-1 $\alpha$  mRNA expression was sustained at >25-fold-increased levels for at least 21 days after intradermal plasmid DNA injection/electroporation. Following the induction of HIF-1 $\alpha$  expression on day 3, levels of VEGF, PLGF, PDGFB, and ANGPT2 mRNA increased on day

7 to levels that were 8-fold to 37-fold higher than baseline levels. ANGPT1 mRNA expression was not induced following gWIZ-CA5 treatment, which is consistent with a proangiogenic response in which the combination of VEGF and ANGPT2 promotes budding of new capillaries (Hanahan, 1997).

A growing body of experimental evidence indicates that angiogenic growth factors/cytokines play several major physiological roles in the response to tissue injury. First, they act on endothelial cells and pericytes within blood vessels surrounding the injured tissue to induce the sprouting of new capillaries to perfuse the wound tissue. Second, they function to mobilize CACs into peripheral blood. CACs are a diverse collection of cell types that subsequently home to the site of injury and promote angiogenesis, either by directly incorporating into neovasculature or indirectly by serving as an additional source of angiogenic growth factors/cytokines. Third, VEGF and other growth factors may have direct effects on keratinocytes (Wilgus et al., 2005). Remarkably, the increased HIF-1 $\alpha$  expression on day 3 after HIF-1 $\alpha$ CA5 gene transduction was accompanied by a >60-fold increase in the number of CACs relative to day 0, demonstrating that HIF-1 $\alpha$ CA5 gene transduction is sufficient to mobilize CACs in diabetic mice. Surprisingly, the peak level of CACs (day 3) preceded the peak levels of mRNAs encoding angiogenic growth factors (day 7), suggesting that the key cytokine(s) responsible for CAC mobilization in response to HIF-1 $\alpha$ CA5 gene transduction in diabetic mouse skin may remain to be identified.

The synergistic activity of multiple angiogenic factors plays a critical role in vascular responses to injury. It is likely that the coordinate induction of genes encoding multiple angiogenic growth factors and the marked CAC mobilization contributed to the significant improvement in angiogenesis and wound healing, which was observed in *db/db* mice that received HIF-1 $\alpha$ CA5 gene therapy. Two other studies, using different wound models, different gene transduction strategies, and different forms of active HIF-1 $\alpha$  have also demonstrated improved wound healing and angiogenesis (Trentin et al., 2006; Mace et al., 2007), although these studies involved non-diabetic and/or young mice. Impaired wound healing in elderly diabetic individuals represents a major cause of morbidity and mortality for which current therapeutic options remain limited. The results of this study provide a scientific foundation for further development of HIF-1 $\alpha$ CA5 gene therapy as a means to overcome age-dependent impairment of wound healing and angiogenesis in the diabetic population.

## Abbreviations

HIF-1, hypoxia-inducible factor 1  
 VEGF, vascular endothelial growth factor  
 ANGPT, angiopoietin  
 PDGF, platelet-derived growth factor  
 PLGF, placental growth factor  
 CAC, circulating angiogenic cell  
 qRT-PCR, quantitative real-time reverse transcription polymerase chain reaction  
 DiI, 1,1'-dioctadecyl-3,3,3',3'-tetramethylindocarbocyanine  
 LDL, low density lipoprotein  
 FITC, fluorescein isothiocyanate  
 BS-1, *Bandeira simplicifolia* agglutinin-1.

## Acknowledgments

This work was supported by funds from the American Diabetes Association, the Hendrix Burn Fund, and The Johns Hopkins Institute for Cell Engineering. Under a licensing agreement between Genzyme Corporation and The Johns Hopkins University, G.L.S. is entitled to a share of fees received by the University from sales of licensed technology. The terms of this arrangement are managed by the University in accordance with its conflict of interest policies.

Contract grant sponsor: American Diabetes Association; Contract grant number: 1-05-RA-50

## Literature Cited

- Albina JE, Mastrofrancesco B, Vessella JA, Louis CA, Henry WL Jr, Reichner JS. HIF-1 expression in healing wounds: HIF-1 $\alpha$  induction in primary inflammatory cells by TNF- $\alpha$ . *Am J Physiol* 2001;281:C1971–C1977.
- Asahara T, Takahashi T, Masuda H, Kalka C, Chen D, Iwaguro H, Inai Y, Silver M, Isner JM. VEGF contributes to postnatal neovascularization by mobilizing bone marrow-derived endothelial progenitor cells. *EMBO J* 1999;18:3964–3972. [PubMed: 10406801]
- Bosch-Marcé M, Okuyama H, Wesley JB, Sarkar K, Kimura H, Liu YV, Zhang H, Strazza M, Rey S, Savino L, Zhou YF, McDonald KR, Na Y, Vandiver S, Rabi A, Shaked Y, Kerbel R, Lavallee T, Semenza GL. Effects of aging and hypoxia-inducible factor-1 activity on angiogenic cell mobilization and recovery of perfusion following limb ischemia. *Circ Res* 2007;101:1310–1318. [PubMed: 17932327]
- Brahimi-Horn MC, Pouyssegur J. Harnessing the hypoxia-inducible factor in cancer and ischemic disease. *Biochem Pharmacol* 2007;73:450–457. [PubMed: 17101119]
- Brem H, Tomic-Canic M, Entero H, Hanflik AM, Wang VM, Fallon JT, Erlich HP. The synergism of age and db/db genotype impairs wound healing. *Exp Gerontol* 2007;42:523–531. [PubMed: 17275236]
- Byrnes CK, Malone RW, Akhter N, Nass PH, Wetterwald A, Cecchini MG, Duncan MD, Harmon JW. Electroporation enhances transfection efficiency in murine cutaneous wounds. *Wound Repair Regen* 2004;12:397–403. [PubMed: 15260804]
- Catrina SB, Okamoto K, Pereira T, Brismar K, Poellinger L. Hyperglycemia regulates hypoxia-inducible factor 1 $\alpha$  protein stability and function. *Diabetes* 2004;53:3226–3232. [PubMed: 15561954]
- Chesnoy S, Huang L. Enhanced cutaneous gene delivery following intradermal injection of naked DNA in a high ionic strength solution. *Mol Ther* 2002;5:57–62. [PubMed: 11786046]
- Cianfarani F, Zambruno G, Brogelli L, Sera F, Lacal PM, Pesce M, Capogrossi MC, Failla CM, Napolitano M, Odorisio T. Placenta growth factor in diabetic wound healing: altered expression and therapeutic potential. *Am J Pathol* 2006;169:1167–1182. [PubMed: 17003476]
- Cummins EP, Taylor CT. Hypoxia-responsive transcription factors. *Pflugers Arch* 2005;50:363–371. [PubMed: 16007431]
- Davidson JM. Animal models for wound repair. *Arch Dermatol Res* 1998;290:S1–S11. [PubMed: 9710378]
- Elson DA, Ryan HE, Snow JW, Johnson R, Arbeit JM. Coordinate upregulation of hypoxia-inducible factor (HIF)-1 $\alpha$  target genes during multi-stage epidermal carcinogenesis and wound healing. *Cancer Res* 2000;60:6189–6195. [PubMed: 11085544]
- Fadini GP, Miorin M, Facco M, Bonamico S, Baesso I, Grego F, Menegolo M, Vigili de Kreutzenberg S, Tiengo A, Agostini C, Avogaro A. Circulating endothelial progenitor cells are reduced in peripheral vascular complications of type 2 diabetes mellitus. *J Am Coll Cardiol* 2005;45:1449–1557. [PubMed: 15862417]
- Fadini GP, Sartore S, Albiero M, Baesso I, Murphy E, Menegolo M, Grego F, Vigili de Kreutzenberg S, Tiengo A, Agostini C, Avogaro A. Number and function of endothelial progenitor cells as a marker of severity for diabetic vasculopathy. *Arterioscler Thromb Vasc Biol* 2006;26:2140–2146. [PubMed: 16857948]
- Ferguson M, Byrnes C, Sun L, Marti G, Bonde P, Duncan M, Harmon JW. Wound healing enhancement: electroporation to address a classic problem of military medicine. *World J Surg* 2005;29:S55–S59. [PubMed: 15815830]
- Forsythe JA, Jiang BH, Iyer NV, Agani F, Leung SW, Koos RD, Semenza GL. Activation of vascular endothelial growth factor gene transcription by hypoxia-inducible factor 1. *Mol Cell Biol* 1996;16:4604–4613. [PubMed: 8756616]
- Frank S, Hubner G, Breier G, Longaker MT, Greenhalgh DG, Werner S. Regulation of vascular endothelial growth factor expression in cultured keratinocytes. *J Biol Chem* 1995;270:12607–12613. [PubMed: 7759509]

- Fukuda R, Hirota K, Fan F, Jung YD, Ellis LM, Semenza GL. Insulin-like growth factor 1 induces hypoxia-inducible factor 1-mediated vascular endothelial growth factor expression, which is dependent on MAP kinase and phosphatidylinositol 3-kinase signaling in colon cancer cells. *J Biol Chem* 2002;277:38205–38211. [PubMed: 12149254]
- Fukuda R, Kelly B, Semenza GL. Vascular endothelial growth factor gene expression in colon cancer cells exposed to prostaglandin E2 is mediated by hypoxia-inducible factor 1. *Cancer Res* 2003;63:2330–2334. [PubMed: 12727858]
- Gosain A, DiPietro LA. Aging and wound healing. *World J Surg* 2004;28:321–326. [PubMed: 14961191]
- Grant MB, May WS, Caballero S, Brown GA, Guthrie SM, Mames RN, Byrne BJ, Vaught T, Spoerri PE, Peck AB, Scott EW. Adult hematopoietic stem cells provide functional hemangioblast activity during retinal neovascularization. *Nat Med* 2002;8:607–612. [PubMed: 12042812]
- Grunewald M, Avraham I, Dor Y, Bachar-Lustig E, Itin A, Jung S, Chimenti S, Landsman L, Abramovitch R, Keshet E. VEGF-induced adult neovascularization: recruitment, retention, and role of accessory cells. *Cell* 2006;124:175–189. [PubMed: 16413490]
- Hanahan D. Signaling vascular morphogenesis and maintenance. *Science* 1997;277:48–50. [PubMed: 9229772]
- Hunt TK, Aslam RS, Beckert S, Wagner S, Ghani QP, Hussain MZ, Roy S, Sen CK. Aerobically derived lactate stimulates revascularization and tissue repair via redox mechanisms. *Antioxid Redox Signal* 2007;9:1115–1124. [PubMed: 17567242]
- Jin DK, Shido K, Kopp HG, Petit I, Shmelkov SV, Young LM, Hooper AT, Amano H, Avecilla ST, Heissig B, Hattori K, Zhang F, Hicklin DJ, Wu Y, Zhu Z, Dunn A, Salari H, Werb Z, Hackett NR, Crystal RG, Lyden D, Rafii S. Cytokine-mediated deployment of SDF-1 induces revascularization through recruitment of CXCR4<sup>+</sup> hemangiocytes. *Nat Med* 2006;12:557–567. [PubMed: 16648859]
- Kelly BD, Hackett SF, Hirota K, Oshima Y, Cai Z, Berg-Dixon S, Rowan A, Yan Z, Campochiaro PA, Semenza GL. Cell type-specific regulation of angiogenic growth factor gene expression and induction of angiogenesis in nonischemic tissue by a constitutively active form of hypoxia-inducible factor 1. *Circ Res* 2003;93:1074–1081. [PubMed: 14576200]
- Kinnaird T, Stabile E, Burnett MS, Shou M, Lee CW, Barr S, Fuchs S, Epstein SE. Local delivery of marrow-derived stromal cells augments collateral perfusion through paracrine mechanisms. *Circulation* 2004;109:1543–1549. [PubMed: 15023891]
- Laughner E, Taghavi P, Chiles K, Mahon PC, Semenza GL. HER2 (neu) signaling increases the rate of hypoxia-inducible factor 1 $\alpha$  (HIF-1 $\alpha$ ) synthesis: novel mechanism for HIF-1-mediated vascular endothelial growth factor expression. *Mol Cell Biol* 2001;21:3995–4004. [PubMed: 11359907]
- Lee PY, Chesnoy S, Huang L. Electroporatic delivery of TGF- $\beta$ 1 gene works synergistically with electric therapy to enhance diabetic wound healing in db/db mice. *J Invest Dermatol* 2004;123:791–798. [PubMed: 15373787]
- Lin MP, Marti GP, Dieb R, Wang J, Ferguson M, Qaiser R, Bonde P, Duncan MD, Harmon JW. Delivery of plasmid DNA expression vector for keratinocyte growth factor-1 using electroporation to improve cutaneous wound healing in a septic rat model. *Wound Repair Regen* 2006;14:618–624. [PubMed: 17014675]
- Loomans CJM, de Koning EJP, Staal FJT, Rookmaaker MR, Verseyden C, de Boer HC, Verhaar MC, Braam B, Rabelink TJ, van Zonneveld AJ. Endothelial progenitor cell dysfunction: a novel concept in the pathogenesis of vascular complications of type 1 diabetes. *Diabetes* 2004;53:195–199. [PubMed: 14693715]
- Mace KA, Yu DH, Paydar KZ, Boudreau N, Young DM. Sustained expression of HIF-1 $\alpha$  in the diabetic environment promotes angiogenesis and cutaneous wound repair. *Wound Repair Regen* 2007;15:636–645. [PubMed: 17971009]
- Marti G, Ferguson M, Wang J, Byrnes C, Dieb R, Qaiser R, Duncan MD, Harmon JW. Electroporative transfection with KGF-1 DNA improves wound healing in a diabetic mouse model. *Gene Ther* 2004;11:1780–1785. [PubMed: 15470477]
- Michaels J, Churgin SS, Blechman KM, Greives MR, Aarabi S, Galiano RD, Gurtner GC. db/db mice exhibit severe wound-healing impairments compared with other murine diabetic strains in a silicone-splinted excisional wound model. *Wound Repair Regen* 2007;15:665–670. [PubMed: 17971012]

- Patel TH, Kimura H, Weiss CR, Semenza GL, Hofmann LV. Constitutively active HIF-1 $\alpha$  improves perfusion and arterial remodeling in an endovascular model of limb ischemia. *Cardiovasc Res* 2005;68:144–154. [PubMed: 15921668]
- Pavselj N, Preat V. DNA electrotransfer into the skin using a combination of one high-and one low-voltage pulse. *J Control Release* 2005;106:407–415. [PubMed: 15982778]
- Pugh CW, Ratcliffe PJ. Regulation of angiogenesis by hypoxia: role of the HIF system. *Nat Med* 2003;9:677–684. [PubMed: 12778166]
- Rehman J, Li J, Orschell CM, March KL. Peripheral blood "endothelial progenitor cells" are derived from monocyte/macrophages and secrete angiogenic growth factors. *Circulation* 2003;107:1164–1169. [PubMed: 12615796]
- Selvin E, Marinopoulos S, Berkenblit G, Rami T, Brancati FL, Powe NR, Golden SH. Meta-analysis: Glycosylated hemoglobin and cardiovascular disease in diabetes mellitus. *Ann Intern Med* 2004;141:421–431. [PubMed: 15381515]
- Semenza GL. Life with oxygen. *Science* 2007;318:62–64. [PubMed: 17916722]
- Semenza GL, Jiang BH, Leung SW, Passantino R, Concordet JP, Maire P, Giallongo A. Hypoxia response elements in the aldolase A, enolase 1, and lactate dehydrogenase A gene promoters contain essential binding sites for hypoxia-inducible factor 1. *J Biol Chem* 1996;271:32529–32537. [PubMed: 8955077]
- Stiehl DP, Jelkmann W, Wenger RH, Hellwig-Bürgel T. Normoxic induction of the hypoxia-inducible factor 1 $\alpha$  by insulin and interleukin-1 $\beta$  involves the phosphatidylinositol 3-kinase pathway. *FEBS Lett* 2002;512:157–162. [PubMed: 11852072]
- Treins C, Giorgetti-Peraldi S, Murdaca J, Semenza GL, van Obberghen E. Insulin stimulates hypoxia-inducible factor 1 through a phosphatidylinositol 3-kinase/target of rapamycin-dependent signaling pathway. *J Biol Chem* 2002;277:27975–27981. [PubMed: 12032158]
- Trentin D, Hall H, Wechsler S, Hubbell JA. Peptide-matrix-mediated gene transfer of an oxygen-insensitive hypoxia-inducible factor-1 $\alpha$  variant for local induction of angiogenesis. *Proc Natl Acad Sci USA* 2006;103:2506–2511. [PubMed: 16477043]
- Wang GL, Jiang BH, Rue EA, Semenza GL. Hypoxia-inducible factor 1 is a basic-helix-loop-helix-PAS heterodimer regulated by cellular O<sub>2</sub> tension. *Proc Natl Acad Sci USA* 1995;92:5510–5514. [PubMed: 7539918]
- Werner S, Breden M, Hubner G, Greenhalgh DG, Longaker MT. Induction of keratinocyte growth factor expression is reduced and delayed during wound healing in the genetically diabetic mouse. *J Invest Dermatol* 1994;103:469–473. [PubMed: 7930669]
- Wetzler C, Kämpfer H, Stallmeyer B, Pfeilschifter J, Frank S. Large and sustained induction of chemokines during impaired wound healing in the genetically diabetic mouse: prolonged persistence of neutrophils and macrophages during the late phase of repair. *J Invest Dermatol* 2000;115:245–253. [PubMed: 10951242]
- Wilgus TA, Matthies AM, Radek KA, Dovi JV, Burns AL, Shankar R, DiPietro LA. Novel function for vascular endothelial growth factor receptor-1 on epidermal keratinocytes. *Am J Pathol* 2005;167:1257–1266. [PubMed: 16251410]
- Yoder MC, Mead LE, Prater D, Krier TR, Mroueh KN, Li F, Krasich R, Temm CJ, Prchal JT, Ingram DA. Redefining endothelial progenitor cells via clonal analysis and hematopoietic stem/progenitor cell principals. *Blood* 2007;109:1801–1809. [PubMed: 17053059]

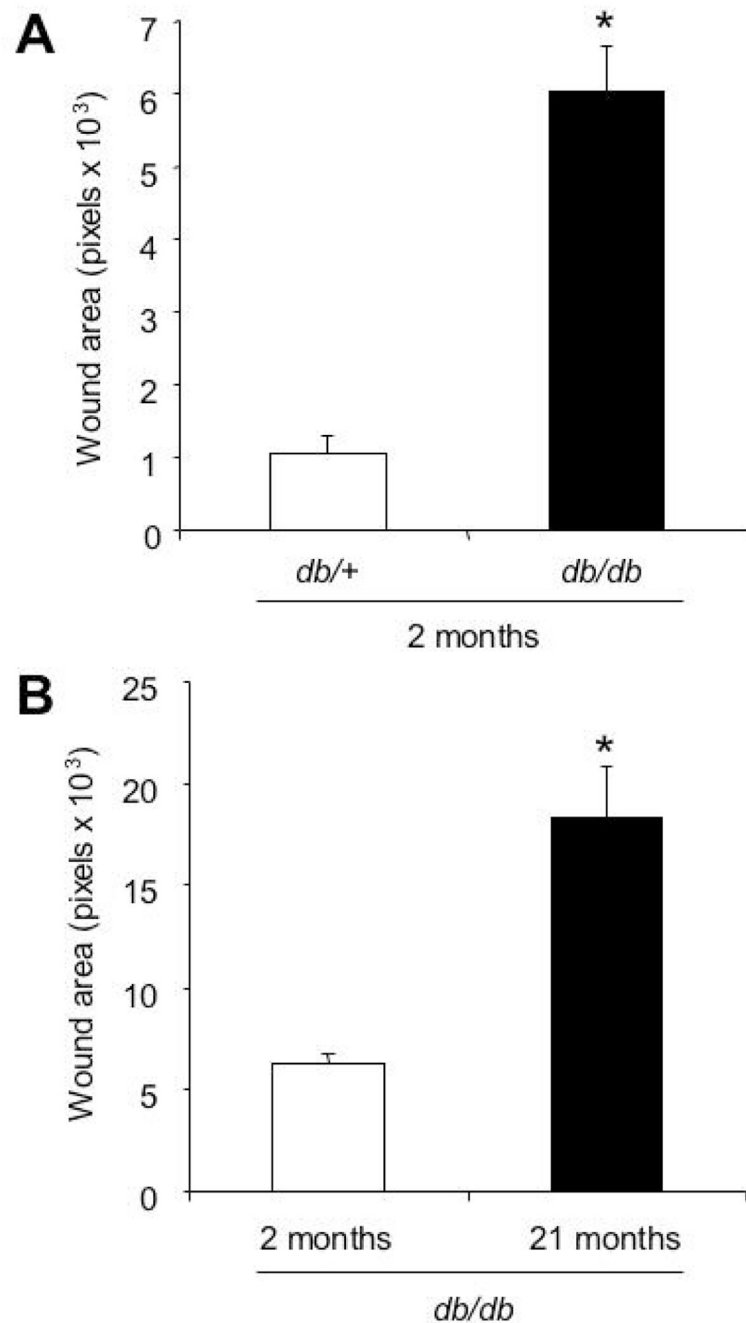


**Fig. 1.** Wound healing characteristics of *db/db* mice. A: Excisional wound closure in 2-month-old diabetic mice (*db/db*) and their heterozygous littermates (*db/+*). The bar graph shows the wound area (in pixels) measured by computer assisted planimetry on day 9 (mean  $\pm$  SEM, n = 20 for each group). \* $P < 0.01$ , Student's t-test. B: The effect of age on wound healing in *db/db* mice. For mice of the indicated age, the bar graph shows wound area on day 9 (mean  $\pm$  SEM, n = 20 for each group). \* $P < 0.01$ , Student's t-test.

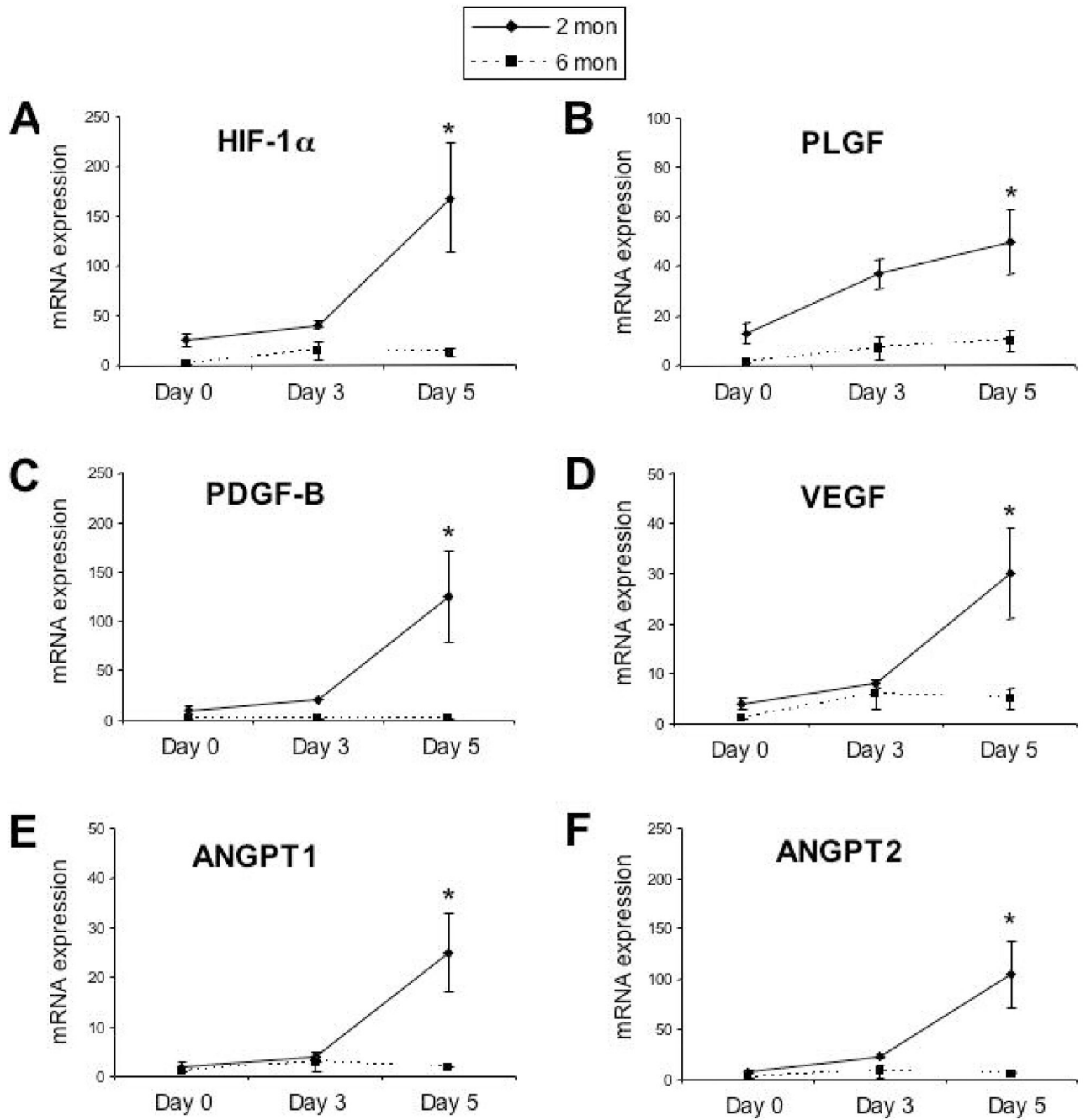


**Fig. 2.** Expression of mRNAs for HIF-1 $\alpha$  and angiogenic cytokines in wounds of 2- and 6-month-old *db/db* mice. Total RNA was extracted from normal skin (day 0) or wounds on day 3 or day 5 and assayed by qRT-PCR for each mRNA. A: HIF-1 $\alpha$ . B: PLGF. C: PDGF-B. D: VEGF. E: ANGPT1. F: ANGPT2. \* $P < 0.01$ , ANOVA with Tukey Test,  $n = 3$  for each group.

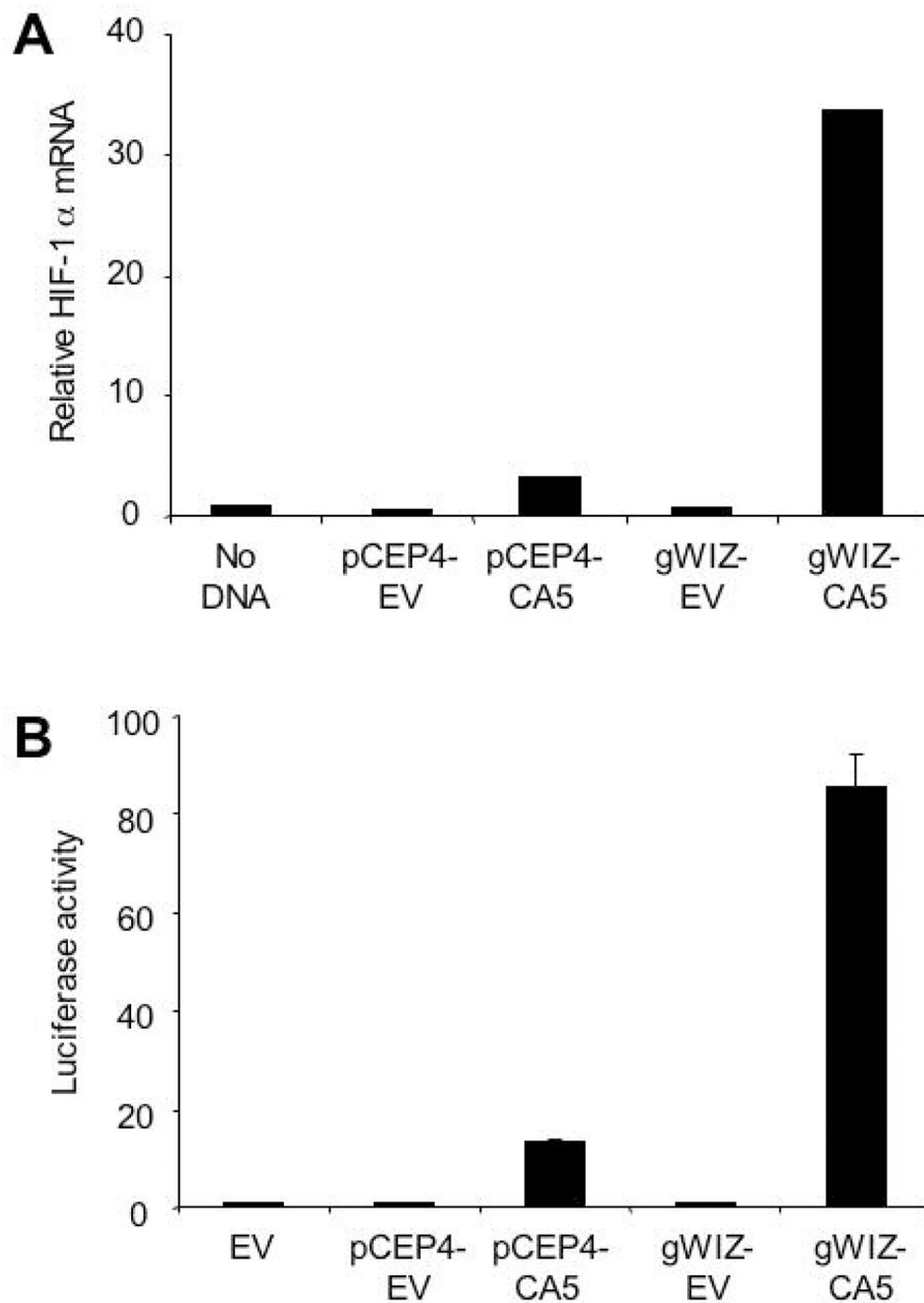


**Fig. 3.** Comparison of expression vectors encoding HIF-1 $\alpha$ CA5. **A:** Analysis of HIF-1 $\alpha$  mRNA levels. HEK-293T cells were transfected with 1  $\mu$ g of pCEP4-CA5, gWIZ-CA5, or empty vector (EV). Total RNA was extracted 24 hours after transfection and assayed by qRT-PCR. The results were normalized to those from non-transfected cells. **B:** Analysis of HIF-1 transcriptional activity. HEK-293T cells were co-transfected with: control reporter pSV-Renilla, encoding *Renilla* luciferase; HIF-1-dependent reporter p2.1, encoding firefly luciferase; and pCEP4-CA5, gWIZ-CA5, or EV. Cells were harvested after 24 hours and the ratio of firefly:*Renilla* luciferase activity was determined. The results were normalized to those from cells transfected with EV (mean  $\pm$  SEM, n = 3 independent transfections for each group).

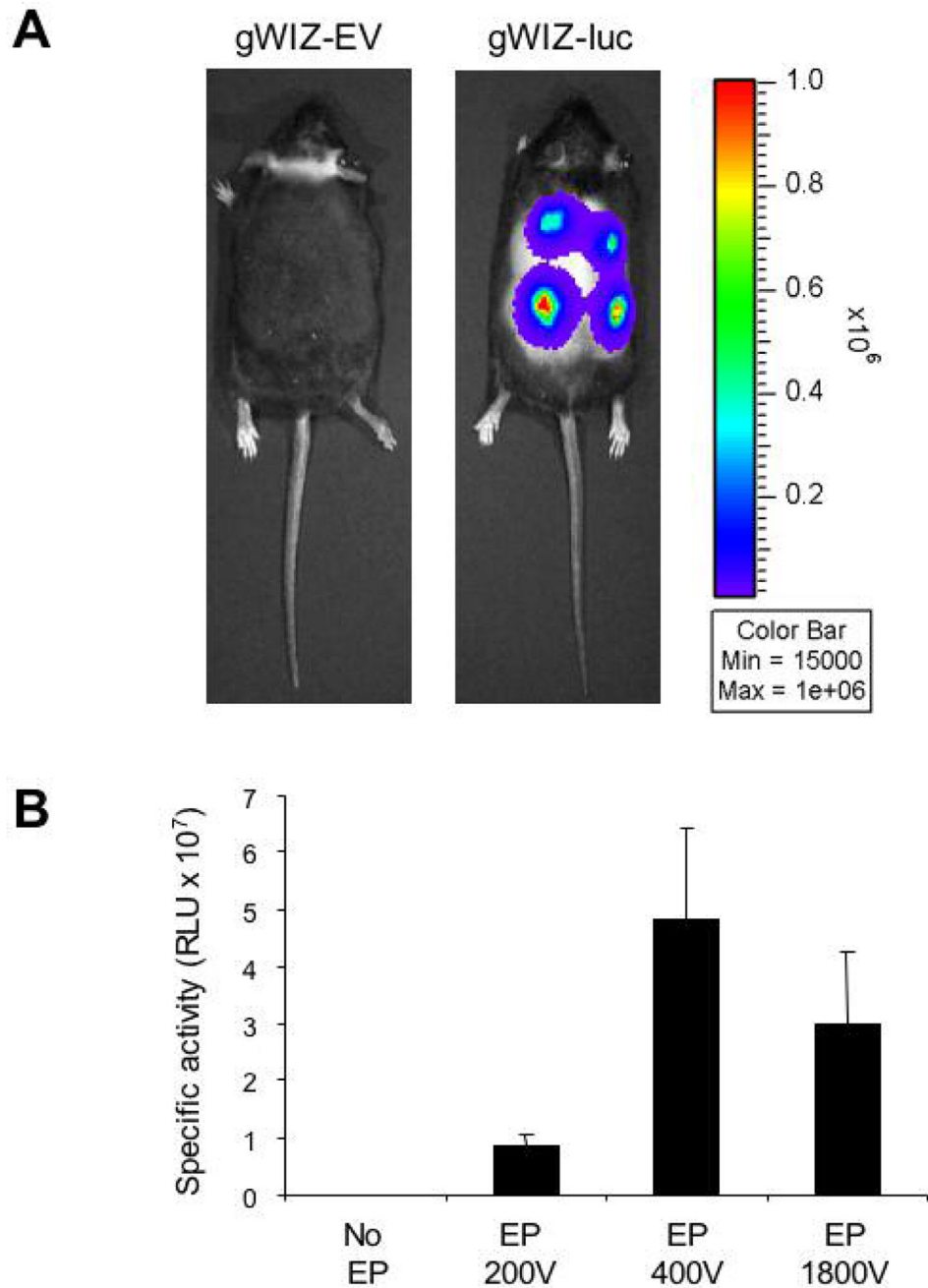


**Fig. 4.** Establishing optimal electroporation parameters for cutaneous DNA delivery. A: Bioluminescent imaging was performed 24 hours after 50- $\mu$ g intradermal injections of gWIZ-EV or gWIZ-luc (encoding firefly luciferase) plasmid DNA followed by electroporation. B: Mean bioluminescence was determined 24 hours after injection of gWIZ-luc plasmid without electroporation (No EP) or followed by electroporation (EP) using 3 different protocols (n = 8 for each group).

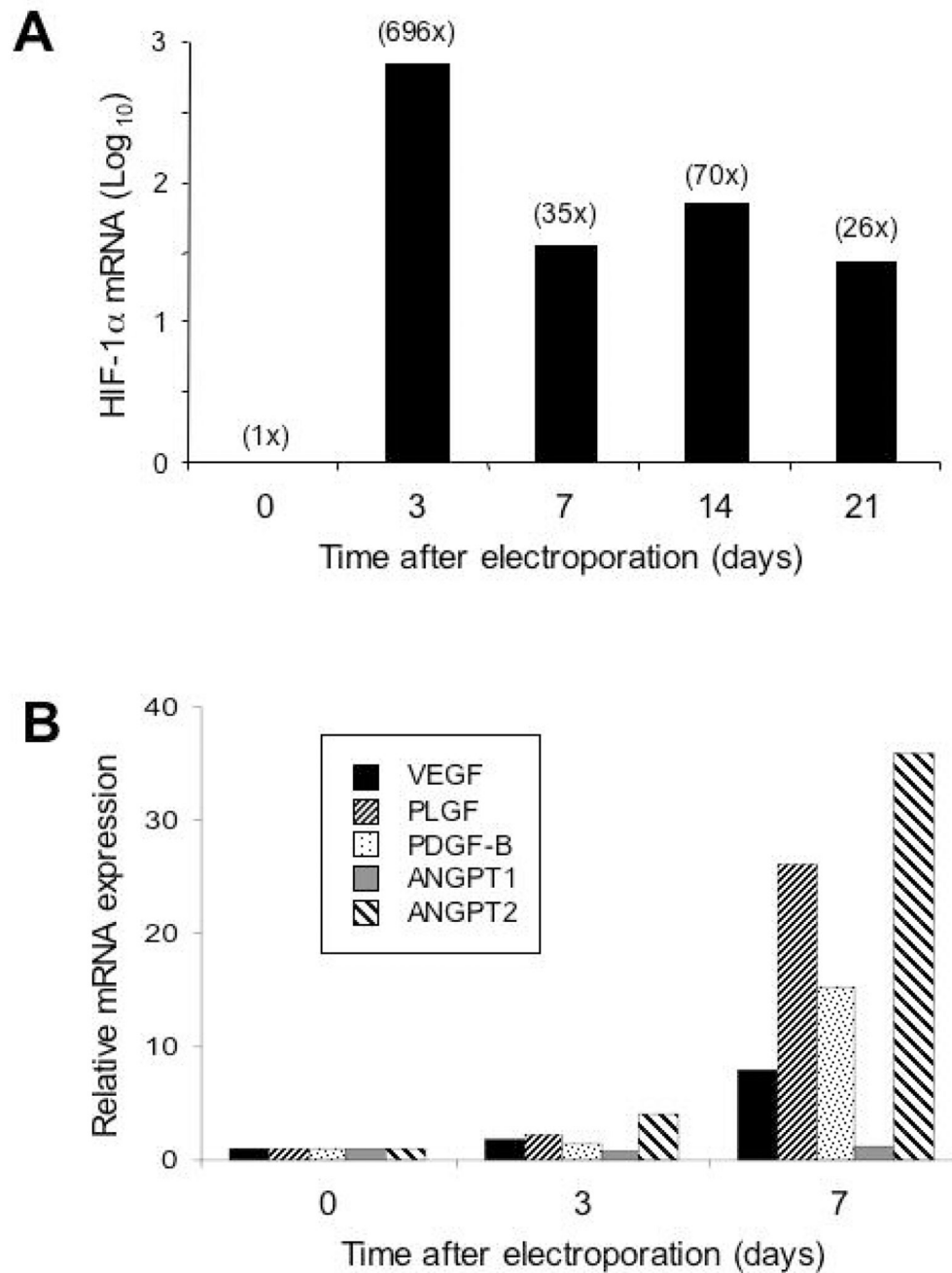


**Fig. 5.** Analysis of mRNA expression following electroporation-facilitated transduction of gWIZ-CA5 into *db/db* mice. RNA was isolated from mouse skin on the indicated day after plasmid DNA injection/electroporation and analyzed by qRT-PCR for mRNAs encoding HIF-1 $\alpha$  (A) and angiogenic cytokines (B).

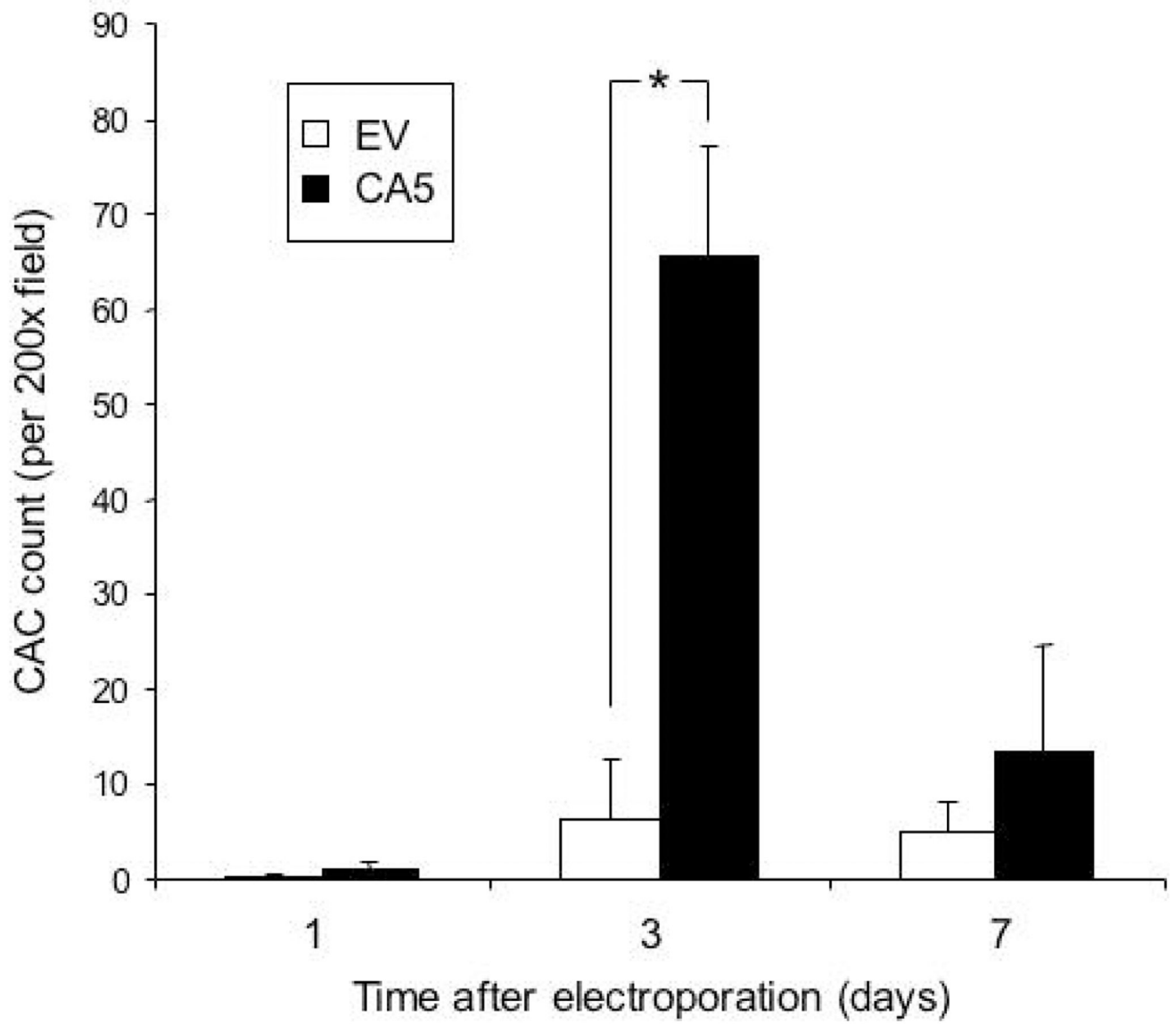


**Fig. 6.** Circulating angiogenic cell (CAC) counts in peripheral blood 1, 3, or 7 days after electroporation-facilitated transduction of gWIZ-CA5 or gWIZ-EV. Peripheral blood from 2 mice was pooled for isolation of mononuclear cells. The cells were cultured for 4 days in the presence of endothelial growth factors and the number of cells per 200x field that internalized DiI-labeled acetylated LDL and bound FITC-labeled BS-1 lectin was determined. The mean number of CACs is shown ( $\pm$  SEM;  $n = 3$  pools each). \* $P < 0.05$ , ANOVA with Tukey Test.

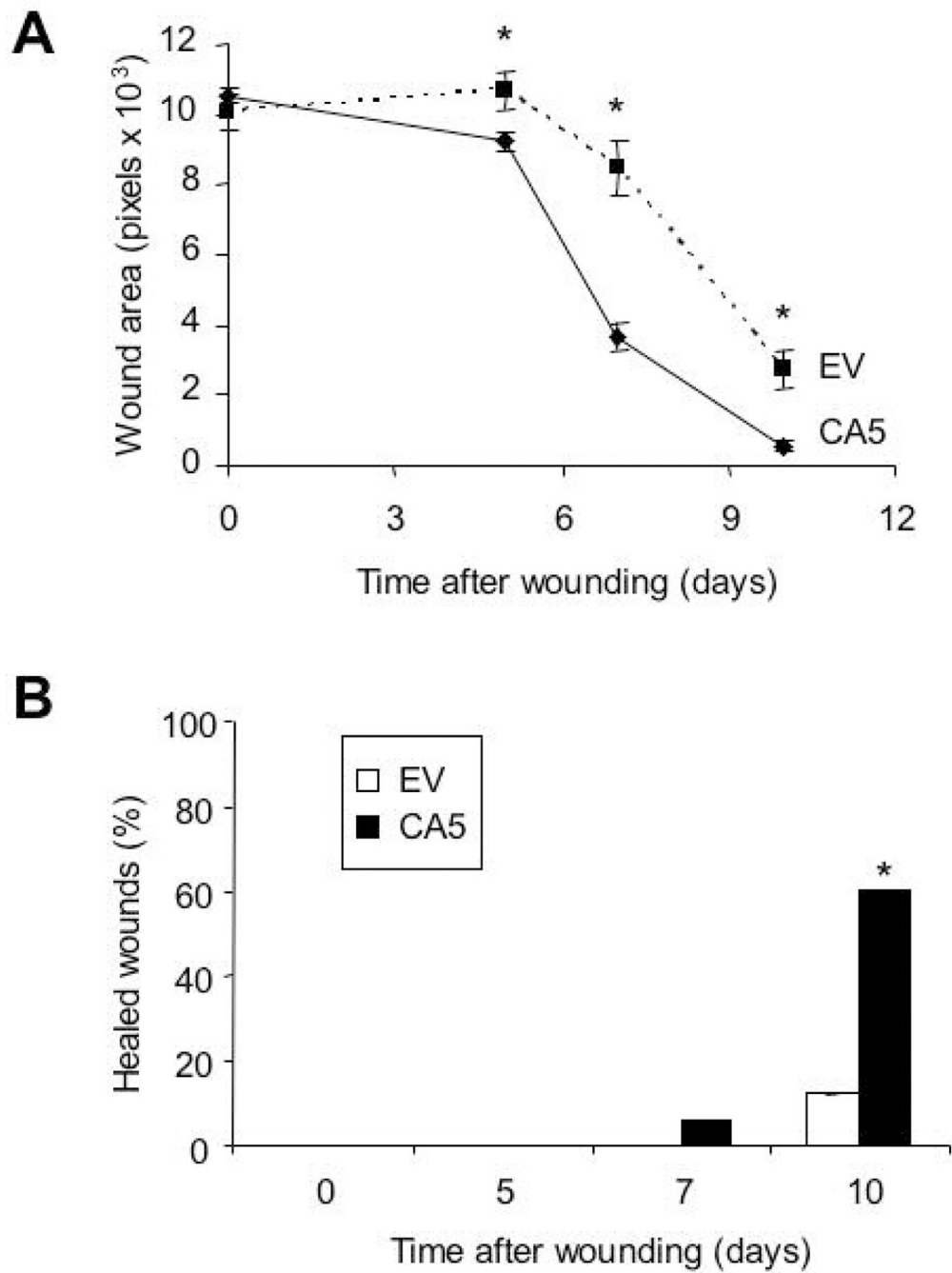


**Fig. 7.** Wound closure in *db/db* mice after electroporation-facilitated DNA transduction. A: Open wound area (in pixels) was determined on the indicated day after wounding and transfection with gWIZ-CA5 (CA5) or gWIZ-EV (EV). Mean  $\pm$  SEM is shown ( $n = 48$  for CA5;  $n = 20$  for EV).  $*P < 0.05$ , ANOVA with Tukey Test. B: Percentage of wounds achieving  $\geq 95\%$  closure after transfection with CA5 vs EV is shown.  $*P < 0.001$ , Mann-Whitney Rank Sum Test.

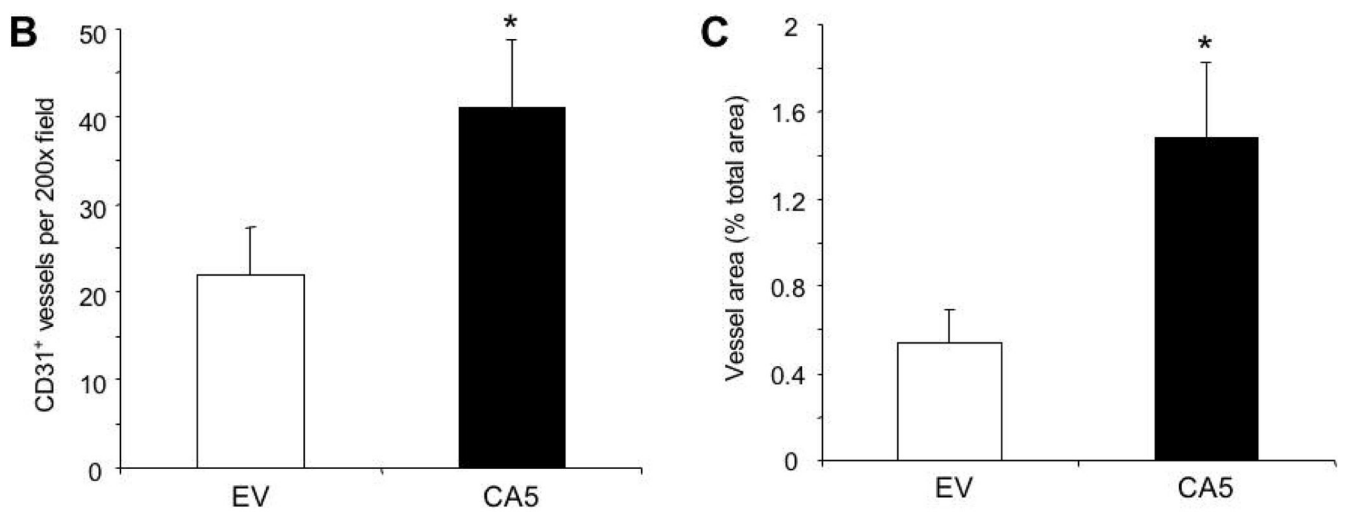
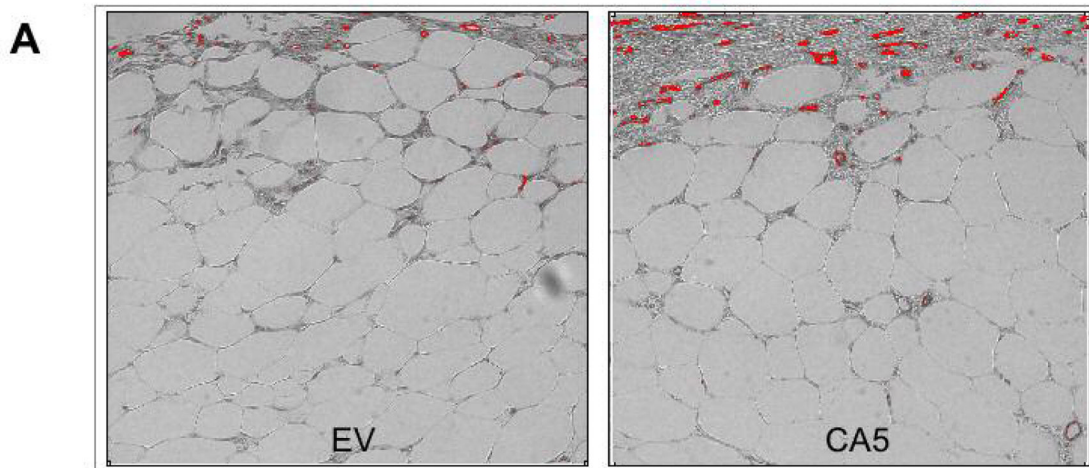


**Fig. 8.** Immunohistochemical analysis of angiogenesis. A: Wounds that were electroporated with gWIZ-EV (EV) or gWIZ-CA5 (CA5) were harvested on day 7, stained with an antibody against PECAM-1 (CD 31), and image analysis was performed to capture the signal (red). B–C: Mean vessel density (number of vessels per 200x field; B) and vessel area (as a percentage of the total area of the field; C) were determined (n = 15 for each group). \* $P < 0.05$ , Student's t-test.